

December 31, 1981

To: ULBA Study Group

From: R. C. Walker

Subject: Draft of Configuration Section

Attached is my current draft of the configuration section of the proposal. The draft should not be considered final and, in particular, the numbers in the tables should not be considered final (Particularly the cost of N station arrays). I am somewhat concerned that the test source used here does not show the differences between arrays as well as it could. Considering the effects of sidelobes that are discussed in the Aperture Synthesis section, I suspect that a source that has real flux in more and more cells as the map gets better would provide a better test of configurations. Any model containing Gaussians would qualify, as would most real sources, and I may try some tests during the second half of January to see if I can more clearly show the differences between arrays. If we stay with the current model, I will need to reexamine some of the rms numbers in the second table because they do not seem to reflect the obvious improvements in the maps with the number of stations in the low declination case. I have distributed the draft in its current form because the text need not change significantly if a different source is used and I will not be able to work on it until after mid January. It would be good to have comments on it by then.

## APERTURE SYNTHESIS

The desired output of the ULBA will usually be a map of a celestial radio source. We can represent that map as a two-dimensional intensity function,  $I(x,y)$ , where  $x$  and  $y$  are angular coordinates on the sky.  $I(x,y)$  can be described in terms of its spatial frequency components,  $U(u,v)$ , by means of the complex, two-dimensional Fourier transform:

$$I(x,y) = \int du \int dv U(u,v) \exp(-i2\pi(ux+vy)) \quad (\text{III-1})$$

where  $u$  and  $v$  are the number of spatial wavelengths per radian in the  $x$  and  $y$  directions respectively. An observation on a single baseline of an interferometer is a measurement of  $U(u,v)$  at a value of  $u$  and  $v$  given by the components of that baseline, measured in wavelengths, in the plane perpendicular to the line of sight to the source (the  $u-v$  plane). The accuracy with which  $I(x,y)$  can be reconstructed depends on the number and sensitivity of observations of  $U(u,v)$  and on the distribution of the observed points in the  $u-v$  plane. Observations of different  $u-v$  points can be obtained both with observations on different baselines and with observations on the same baseline at different times, allowing the Earth's rotation to change the orientation of the  $u-v$  plane relative to the baseline. With sufficient observations,  $I(x,y)$  can be reconstructed using Equation III-1. The technique is known as aperture synthesis and is used by all radio interferometers including the ULA.

A complication, especially for ULBI, is that an observed value of  $U(u,v)$  is the true value times the geometric mean of the complex gains of the two interferometer elements used to make the measurement. Those gains are often difficult to calibrate and, for ULBI, the phase parts of those gains may be impossible to calibrate. However, the gain of each element affects the observations on all baselines to that element equally. The number of baselines ( $N(N-1)/2$ ) is much larger than the number of elements ( $N$ ) for interferometers with more than a small number of elements. Techniques have been developed to iteratively solve for the gains and the source structure and those techniques are in routine use for current ULBI, MTRLI, ULA, and Westerbork observations.

The most important contributions to the noise in an interferometer map come from random noise in the data, from noise due to calibration errors and from fluctuations in the map due to sidelobes. The random noise in the data is a function of the gain and system temperature of each telescope and is reduced with the square root of the number of data points. The noise due to calibration is proportional to the fractional

calibration error times the correlated flux density of each data point and is only reduced by the square root of the number of independent calibration errors. That number will be at least the number of telescopes and will be larger if there are calibration fluctuations as a function of time because of, for example, weather. The sidelobes are a result of incomplete sampling of the  $u-v$  plane and are a function of the configuration and of the source being mapped. In addition to noise, the map produced by an interferometer can be in error if important spatial frequencies are missed. This is most commonly seen when a source contains extended emission regions that are resolved on the shortest baselines. It is important, therefore to have a wide range of baseline lengths.

The sidelobes are the factor most seriously affected by the configuration so it is worth considering their effects more carefully. The interferometer beam is the map of a point source that is made using Equation III-1, noiseless data, and the  $u-v$  coverage of the interferometer. Such a beam has fluctuations throughout the field which are the sidelobes. A map of a real source consists of the actual distribution of emission in the source convolved with the beam and disturbed by noise. The point-source-subtraction algorithm, CLEAN, is commonly used to remove the sidelobes due to much of the source by iteratively subtracting the beam, scaled to a fraction of the flux density and centered on the location of the highest point in the map remaining after the previous iteration (the residual map). A final map is produced by adding a smooth Gaussian that approximates the central lobe of the beam to the final residual map at the location of each subtracted point. After CLEAN, the rms 'noise' due to sidelobes is approximately equal to the square root of the sum, over all independent pixels (beam areas) in the residual map, of the squares of the real source flux density (as opposed to sidelobes from other pixels) times the rms sidelobe level in the beam. For complex sources, this noise level can be very much larger than the sidelobes in the beam and, in fact, limits the observations to sources (or residual maps) with roughly equal real flux density in a number of pixels independent that is smaller than about the square of the inverse of the rms sidelobe level in the beam. Clearly, it is important to minimize the sidelobes to the greatest degree possible.

## ARRAY CONFIGURATION

The number and location of antennas in the ULBA should be chosen to optimize the ability to make high resolution maps by the procedure

described above at a reasonable cost. Several specific performance goals can be defined that help guide the selection of a configuration. The number of antennas is the most critical parameter that determines the ability of the Array to meet those goals. The location of the antennas is less critical since many configurations with the same number of antennas provide similar performance. The final choice of configuration is likely to depend strongly on factors such as the availability of land, personnel, transportation, and local support. The locations of the antennas in a particular configuration are chosen together to provide reasonable coverage of the  $u-v$  plane. Therefore, any change in the location of one antenna by more than a few kilometers may necessitate changes in the locations of several other antennas or may even force the choice of an entirely different configuration. A final configuration cannot be chosen until the feasibility of many possible sites has been checked. The configurations presented later in this section are meant to be examples that allow reasonable estimates to be made of the cost and performance of the Array. The final configuration may be superior to those presented here but, unless the basic constraints under which the examples were chosen are changed, the differences will be small.

The performance goals and their implications are:

1. The configuration should provide good two-dimensional images for all sources north of the galactic center at  $-28$  degrees declination. This requires the use of north-south as well as east-west baselines. It is difficult to define 'good' precisely because image quality is affected by many factors. However, it should be possible to make images of strong, moderately complex sources over most of the sky in which features one percent as strong as the strongest feature in the map can be believed. (See note later on dynamic range.)

2. Most, if not all, elements should be on United States territory in order to minimize complications in shipping and travel. It might be worth relaxing this constraint slightly to obtain the long north-south spacings provided by stations in Canada and Mexico.

3. The resolution should be as high as possible. This is best accomplished with elements in Hawaii and the East Coast or Puerto Rico. Elements in Europe would provide baselines of similar length but, because of the high latitude of Europe, provide very poor coverage at low declinations. An increase in resolution of about 20% could be obtained with elements near the equator but the cost is probably prohibitive. For maximum north-south resolution, elements should be located in Alaska and Hawaii or in Puerto Rico and New England. The former provides a longer baseline but cannot see as far south as the latter and may be more expensive.

4. The  $u-v$  coverage should be as uniform as possible although it may be "centrally condensed" in the sense that the  $u-v$  coverage

at short spacings might be more complete than at long spacings. This type of coverage facilitates the study of spectral distributions and observations of sources containing bright regions together with relatively extended structure. It is also desirable to have the u-v coverage of a short observation, or "snap-shot", be well distributed. Redundant baselines should be avoided because they reduce the total amount of information obtained on a source and they are not required by the mapping methods that solve for gains along with source structure.

5. The minimum spacing should be less than 200 km. Thus the ULBA will complement the existing Multi-Telescope-Radio-Linked-Interferometer at Jodrell Bank and possible future extensions of the VLA. With a minimum spacing of 200 km and a maximum spacing of 8000 km, 40 ideally distributed baselines are required for complete u-v coverage at high declination. The number of baselines required is increased by a factor of about 3 in order to obtain complete coverage at low declinations and by a small factor that accounts for the difficulty of obtaining ideally distributed baselines. On the other hand, the number of required baselines is reduced by the geographic limitation of north-south baselines to about 4000 km and by the acceptability of a "centrally condensed" configuration. Ten elements, providing 45 baselines appears to be barely sufficient to meet the coverage goals.

6. The array should interact well with the VLA both when the VLA is used for its large collecting area and when information over a wide range of scale sizes is desired. The baselines between the VLA and ULBA elements have about 5 times the sensitivity of other ULBA baselines. To exploit this sensitivity, these baselines should be well distributed in the u-v plane. To accomplish this, the ULBA's major concentration of telescopes should be near the VLA. The closest antenna to the VLA should be about 100 km away from the VLA in order to help fill the gap between the longest VLA spacing (35 km) and the shortest ULBA spacing (200 km).

7. Where practical, elements should be located at high, dry sites for improved high frequency performance. Again, sites in the West are preferred.

8. Each element should be near a major transportation center to facilitate shipping of tapes and access by Array personnel from the operations center. It may also be advisable to site elements at existing observatories or interested universities to take advantage of local technical support.

The constraints listed above help fix several elements of the array. For maximum east-west extent, A station should go in Hawaii, probably near the astronomical facilities on the island of Hawaii

or near Honolulu, and another station should go in Puerto Rico, probably at the Arecibo observatory, or in New England, probably at the Haystack Observatory. For the greatest north-south resolution, a station should go in Alaska, probably near Anchorage where there is transportation and a relatively mild climate, or stations should go in New England and in Puerto Rico. A station should be near the ULA although far enough away to provide interesting short spacings when used with the ULA. Socorro is a possibility. Big Pine, California (Owens Valley Radio Observatory); Green Bank, West Virginia (NRAO); and Westford, Massachusetts (Haystack Observatory) are attractive sites because of the presence of existing radio astronomy facilities and of a strong commitment to ULBI. The desire for good north-south coverage suggests that stations should go at the northern and southern extremes of the contiguous 48 states - eg in Texas or Florida and somewhere near the Canadian border.

The number of elements that the array should include must be chosen on the basis of a trade-off between the quality of the images that can be produced and the cost of the array. It is desirable to have a large number of elements, distributed to provide a wide range of baseline lengths and reasonably complete coverage of the u-v plane in order to minimize sidelobes and produce high quality images. It is also desirable to have a large number of elements in order to make the ratio of the number of observations to the number of unknown gains - as high as possible. However, each additional element requires more expenditure for construction and raises the operating costs. Relative to a linked interferometer such as the ULA, the ULBA would require more elements to provide equivalent coverage over as large a range of scale sizes in the u-v plane because the elements cannot be moved, because ideal configurations such as the ULA's wye, with the desired maximum baselines, will not fit in available territory, and because the time during which a source can be seen on any given baseline is limited by the requirement that it be up at two sites at very different longitudes. However, each element is more expensive to construct and operate than a ULA element because of the large distances between them and because operating personnel are required at each one.

As discussed under point 5 above, 10 elements appears to be the minimum number required to obtain the required u-v coverage. Table III-1 shows several other parameters that should be considered in selecting the number of antennas. The first two columns give the number of stations and the number of baselines. Note that the number of baselines, which determines the number of points in the u-v plane that are sampled, rises with the square of the number of stations so each additional station provides a large increase in information. The third column gives the minimum spacing for an ideal, zero redundancy

array with a maximum baseline of 8000 km. While such an array is impossible, the points discussed in point 5 suggest that an array with the listed minimum spacing can provide acceptable coverage. The fraction of the total information in an observation that can be recovered if the iterative gain solution techniques must be used on both amplitudes and phases is given in column 4. Column 5 lists estimates of the total array cost obtained by scaling the cost of a 10 station array. Note that there may be serious errors for numbers of stations greatly different from 10 for which the whole array design might be different. The final three columns give information on the performance of the array. Column 6 gives the signal-to-noise in a gain solution as a fraction of the signal-to-noise in an individual data point. Columns 7 and 8 give the RMS noise level for the whole array at 5 GHz in a coherence time and in a full 12 hour observation. Figure III-2 shows the ability of an array of 10 stations (Array 2 discussed below) to map a complex source with total assumed flux densities of 10 Jy, 1 Jy, and 100 mJy at a declination of 44 degrees. At 10 Jy, the dynamic range of the map, without further CLEANing, is set by the sidelobes. At 100 mJy, the limit is noise. Figure III-3 shows the ability of the four arrays described below to map the same source (1 Jy) at a declination of -18 degrees. These maps clearly show the differences in performance between 8, 10, and 12 station arrays. A similar test at 44 degrees declination shows approximately the expected differences in rms noise levels but, with the very much better u-v coverage, all the maps were good and the differences were not as apparent as in the low declination case. The model used in these tests is the stronger regions of a scaled down version of a map of MB7 made by Dr. Frazier Owen using xx antennas during the construction of the ULA. All maps are made from fake data based on the model shown and should not be compared to better ULA maps of MB7 that might become available. Parameters describing the performance of the arrays for the tests described here are given in Table III-3. The increase in sensitivity and decrease in sidelobe level with number on antennas are about as expected. Note that in these tests, features containing much less than one percent of the total flux density can be believed but, because of the lack of any one feature containing more than about five percent of the total flux density and because of limits set by receiver noise, the ratio of the brightest feature to the weakest believable features (five times rms) is about 50 for the 1 Jy model. The ratio of 100 suggested earlier as desirable is obtainable with these arrays with simpler sources, with stronger sources (eg the 10 Jy model), and with sources containing a more dominant component (such as Daisy of the Caltech and NRAO design studies).

None of the above parameters provides a clear indication of the

ideal number of elements. With less than nine elements, the fraction of information that can be recovered when gain solutions are used gets uncomfortably low, the minimum spacing gets uncomfortably large and the low declination coverage gets uncomfortably poor. Ten elements appears to provide a reasonable trade-off between performance and cost and this proposal based on a ten element array. A larger number of elements could be obtained for some projects, particularly at the longer wavelengths, through joint observations with pre-existing observatories or with VLB instruments that may be built in Canada and/or Europe. Also, the site near the ULA will be chosen so that the range of baselines available is extended when the ULA is used.

Figures III-4 to III-7 show the u-v coverage for four possible configurations. The scales of the plots are in km in order to be independent of observing frequency. The declinations for which the coverage is shown are chosen to be the centers of strips, each containing 10% of the total area of the sky. Figures III-4 and III-7 show the coverage for the 8 and 12 station arrays that were used in the demonstrations of array capabilities in Figure III-3. Figures III-5 and III-6 show two 10 station arrays that demonstrate the effects of alternative ways of obtaining the reasonable coverage. The array of Figure III-5 has been more carefully optimized than the others, although under the constraint that Owens Valley, Green Bank, and Haystack are included. It could be the final configuration but, more likely, it will be replaced by some other, slightly better, configuration found by ongoing configuration studies. The performance and cost of other good 10 station arrays are not likely to differ significantly from that of the array of Figure III-5, so that array has been used throughout this proposal when a specific configuration has been addressed. Figure III-7 shows the coverage for the array of Figure III-5 for a one hour observation such as might be used in survey experiments.

-----  
FOOTNOTE ON DYNAMIC RANGE

The "dynamic range" is commonly used as a measure of the quality of maps and, in the context of array configuration studies, of the quality of arrays. Several different definitions of dynamic range are used so one must be careful in comparing numbers from different sources. Two common definitions used in array studies are the ratio of the peak flux density per beam to the largest error in the map (used on maps made with fake data based on a known source) and the ratio between the peak flux density and the flux density of the smallest believable feature (about five times the rms noise) in the map. Ideally, the two definitions should produce similar values but the former often produces lower values, partly because gridding problems can be important.



Ultimately, dynamic ranges may provide good criteria for selecting a configuration but great care must be exercised to make certain that the calculated values are not too strong a function of the model and the mapping techniques used in the tests. In this proposal, we have not used dynamic range for comparison of arrays because we are not certain that the technique dependent effects have been removed. However, it is clear that the tested arrays, with sources of intermediate complexity and containing a feature with a large fraction of the total flux density (such as Daisy of the design studies), provide dynamic ranges in excess of 100 over most of the sky.

TABLE III-2

## Functions of the Number of Telescopes

Number of Elements	Number of Baselines	Minimum Baseline -1- km	Fraction of data in closure parameters	Cost of Array -2- M\$	S/N of gain vs data S/N	RMS in sol coherence time mJy <sup>?</sup>	RMS in full track mJy
6	15	533	0.63	28.1	0.41	2.6	0.33
7	21	381	0.69	30.1	0.38	2.2	0.28
8	28	286	0.73	33.6	0.35	1.9	0.24
9	36	222	0.76	36.7	0.33	1.7	0.21
10	45	178	0.79	39.1	0.32	1.5	0.19
11	55	145	0.81	41.9	0.30	1.4	0.17
12	66	121	0.83	44.7	0.29	1.2	0.16
13	78	102	0.84	47.5	0.28	1.1	0.14
14	91	88	0.85	50.4	0.27	1.05	0.13
20	190	42	0.90	67.8	0.22	0.72	0.09
27	351	23	0.92	88.8	0.19	0.53	0.07

1. Assumes high declination and perfect (impossible) uniform spacing of baselines. Note minimum spacing of a VLA configuration of this size would be about 250 km (?). The VLA was designed for uniform coverage at all declinations.
2. Scaled from 10 station array using formula  $12.05 + 2.63*N + .008*N**2$

TABLE III-3

## TEST RESULTS

Array Figure of u-v plot	Number of stations	Model source dec. (Degrees)	RMS sidelobe level (percent)	Total model flux den (Jy)	Peak flux den per beam (mJy)	RMS noise in map (mJy)
III-5	10	44	1.8	10.0	523	0.91 -1-
III-5	10	44	1.8	1.0	52.5	0.22
III-5	10	44	1.8	0.1	5.2	0.17 -2-
III-4	8	44	2.4	1.0	52.6	0.26
III-6	10	44	1.7	1.0	53.1	0.22
III-7	12	44	1.5	1.0	52.3	0.19
III-4	8	-18	4.1	1.0	50.1	0.23 -3-
III-5	10	-18	3.5	1.0	53.8	0.22
III-6	10	-18	3.1	1.0	51.8	0.21
III-7	12	-18	2.7	1.0	53.3	0.23

1. The noise in the 10 Jy map is dominated by sidelobes. As with all the other maps, the CLEAN was taken for 2000 iterations. If it had been extended, the noise level would probably be lower.
2. The noise in the 0.1 Jy map is dominated by noise in the data. The configuration will be relatively unimportant in this case.
3. (\*\*\*\*\* I need to find out why the -18 deg rms values do not reflect the quality of the maps \*\*\*\*\*)

## FIGURE CAPTIONS

### FIGURE III-2

These maps show the ability of a 10 station ULB Array to map a fake source with a total flux density of 10, 1, and 0.1 Jy. The array used is the one described in Figure III-5. The model, which is shown at the upper left, consists of the strongest 1371 pixels of a map of MB7 made with the ULA while it was under construction. As with all of the maps displayed in this section, the test maps should be compared with the model, not with any better maps of MB7 that might now be available. The model has been scaled in size and flux density to be appropriate for the ULB tests. The 10, 1 and 0.1 Jy maps are in the center left, center right, and lower left panels, respectively. The contours in all these maps are at the -12, -6, -3, -1.5, -0.5, 0.5, 1.5, 3, 6, 12, 24, 48, and 96 percent levels relative to the strongest feature in the map. Note the factor of two increase between each of the levels. The lower right panel shows the 0.1 Jy map with the -1.5, -0.5, 0.5, and 1.5 percent contours removed to more clearly show the structure that was successfully mapped. All of the maps have been made using the same restoring beam after CLEAN to facilitate comparison even though there are very small differences between the actual beams. That restoring beam is an elliptical Gaussian with a full width at half maximum of 1.56 by 1.43 milli arcseconds with the major axis in position angle -31 degrees.

### FIGURE III-3

These maps show the ability of the four arrays presented in Figures III-4 to III-7 to map the model source at a declination of -18 degrees. Again, the model source is shown in the upper left. The maps in the center left, lower left, center right, and lower right are produced using the arrays from Figures III-4, III-5, III-6, and III-7 respectively. The contour levels are the same as in Figure III-2. At the lower declinations, the beams of the different arrays differ significantly so the fitted beams are used for each map. The full width half maxima and position angles, in milliarcseconds and degrees, for the four beams are (3.16 x 1.21, -5), (3.09 x 1.31, -14), (3.08 x 1.06, -7), (3.38 x 1.32, 1). The model has been convolved with the beam of the first map.

### FIGURE III-4

These plots show the locations of the data points in the u-v plane

that would be obtained with an eight station array having elements at Arecibo, Puerto Rico; Westford, Mass.; North Liberty, Iowa; Las Vegas, New Mexico; Socorro, New Mexico; Las Vegas, Nevada; Great Falls, Montana; and near Mona Kea, Hawaii. The source is observed for the entire time that it is above 10 degrees elevation at any two stations. The different panels show the coverage at declinations, as labeled, that are the centers of declination strips that each contain ten percent of the total area of the sky. The scale of the plots is in km in order to be independent of frequency. Note that the constraints that the minimum baseline be about 200 km and the maximum baseline be about 8000 km lead to rather non-uniform coverage with only 8 stations. For this array, the longest north-south baseline is from Puerto Rico to Mass. and the shortest baseline is between the two stations in New Mexico. There are existing observatories at or near the Arecibo, Westford, North Liberty, and Socorro sites.

FIGURE III-5

This figure shows the u-v coverage for a 10 station array with stations at Westford, Mass.; Green Bank, West Virginia; Grand Fork, North Dakota; Boulder, Colo.; Las Alamos, New Mexico; Socorro, New Mexico; Brownsville, Texas; Big Pine, Calif.; Anchorage, Alaska; and near Mona Kea, Hawaii. The Westford, Green Bank, Socorro, and Big Pine stations are at existing radio astronomy observatories. The long north-south baseline in this array is from Hawaii to Alaska and the short spacing is in New Mexico. This is the array used for costing purposed throughout this proposal. It is derived from Array D2 of the NRAO design study.

FIGURE III-6

This is the u-v coverage for another 10 station array with stations at Arecibo, Puerto Rico; Bangor, Maine; North Liberty, Iowa; Laredo, Texas; Pueblo, Colo.; Southwest of the ULA, New Mexico; Tuscon, Arizona; Spokane, Wash.; Hilo, Hawaii; and Kauai, Hawaii. This array has two stations in Hawaii which might be useful for calibration. With only one in Hawaii, there are no short baselines to that station and it may be difficult to determine the amplitude calibration. There are existing observatories at the Arecibo, North Liberty, ULA, and Tuscon sites.

FIGURE III-7

This shows the u-v coverage for a 12 station array with stations at Arecibo, Puerto Rico; Westford, Mass.; North Liberty, Iowa; Laredo, Texas; Boulder, Colo.; Socorro, New Mexico; Boise, Idaho; Salem, Oregon; Big Pine, Calif.; Goldstone, Calif.; Anchorage, Alaska; and near Mona Kea in Hawaii. The short spacing is in California and the long north-south spacing is from Hawaii to Alaska. There

are existing observatories at the Arecibo, Westford, North Liberty Socorro, Big Pine, and Goldstone (NASA) sites. This array is Array 13 of the Caltech design study with stations added at Socorro and Arecibo.

FIGURE III-8

This figure shows the  $u-v$  coverage that would be obtained with a short observation (one hour) using the array from Figure III-5. Observations of this type, or a small number of such observations at different times, will form a common observing mode for surveys and other projects that don't require high quality maps.

Figure III-2

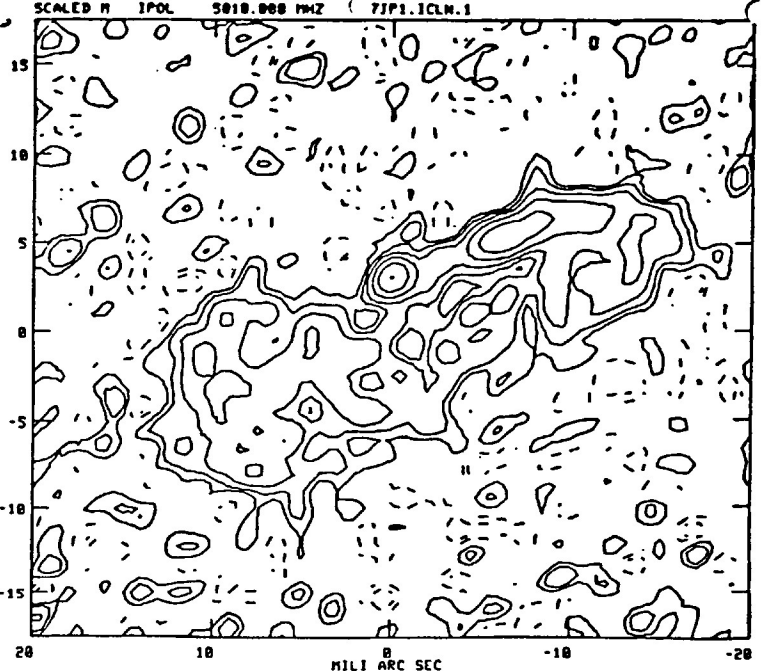
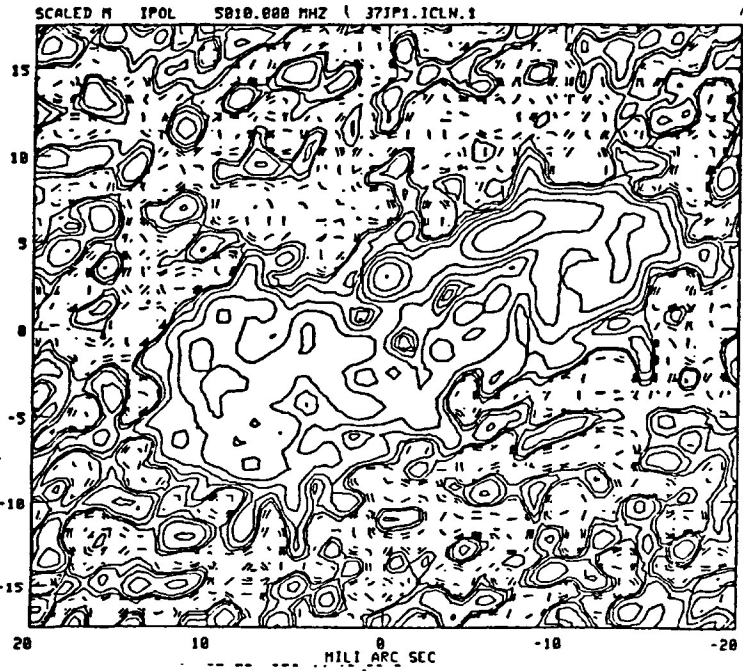
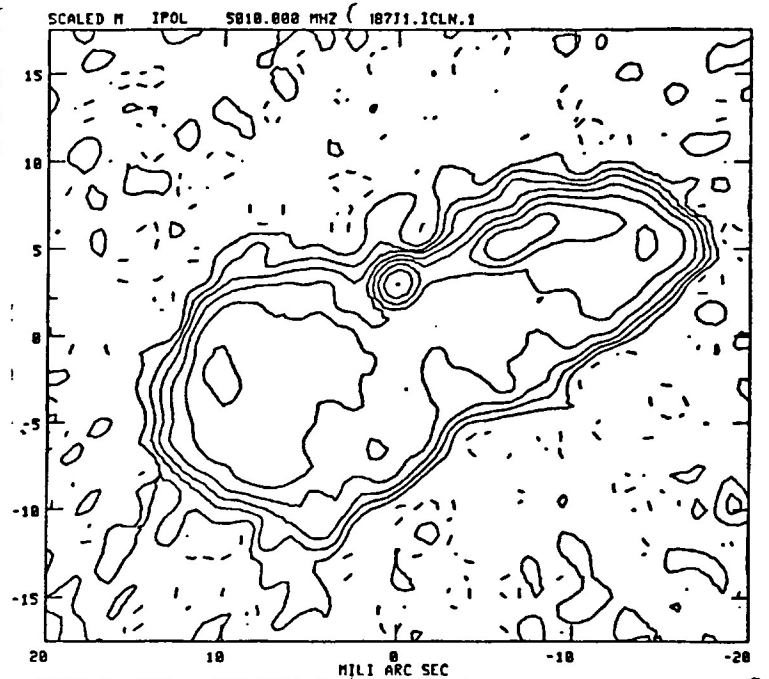
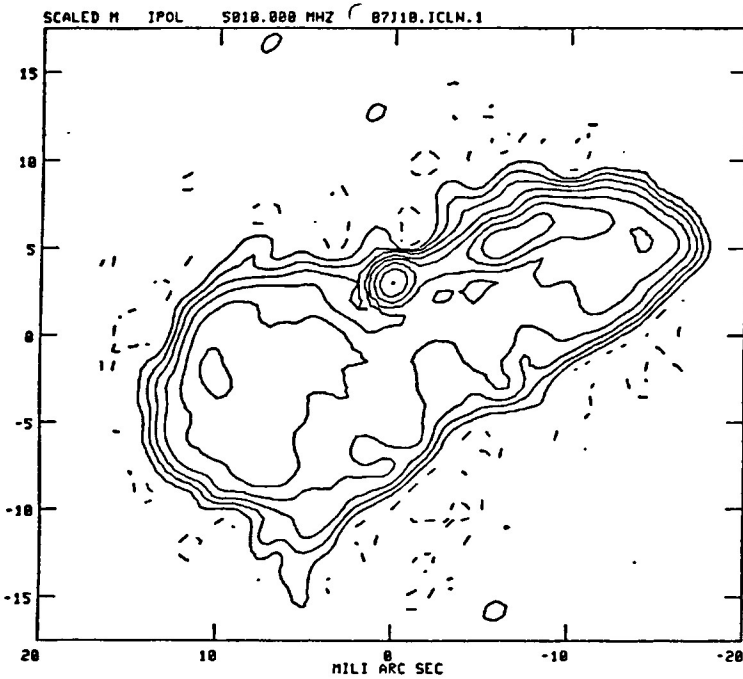
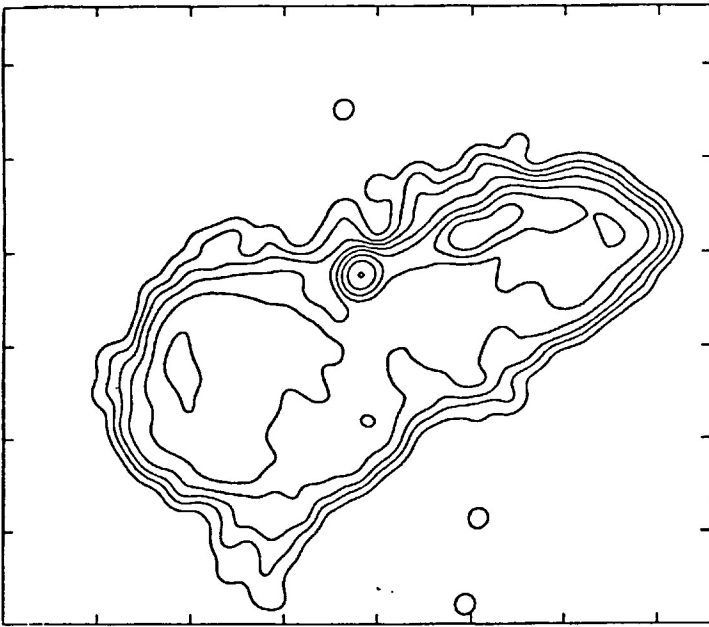
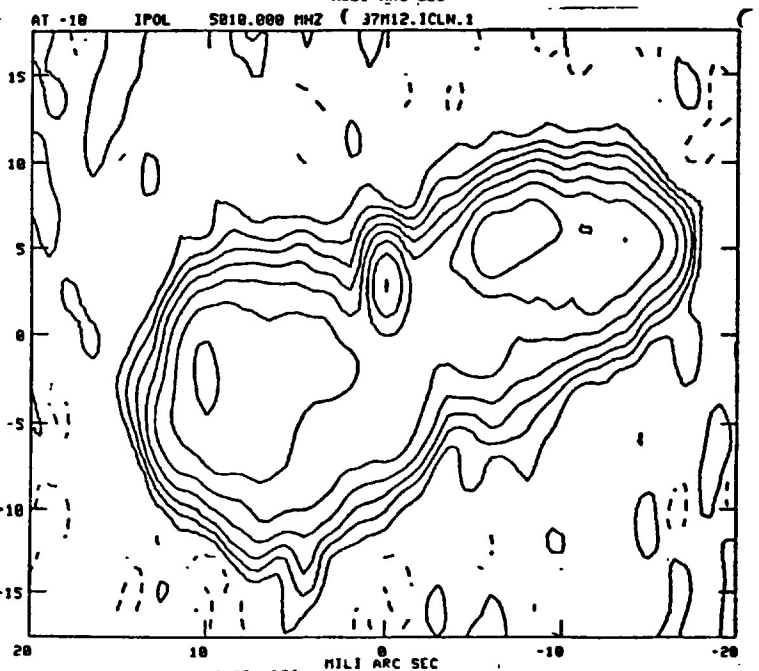
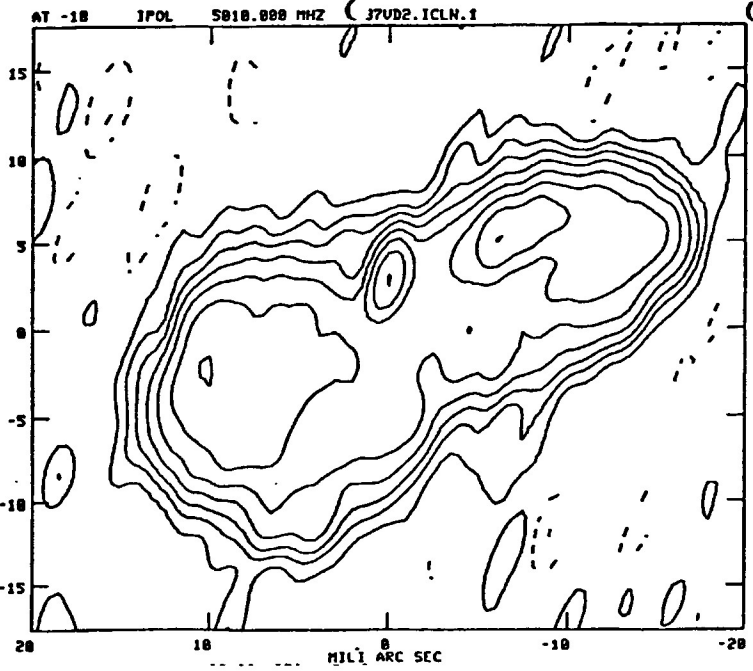
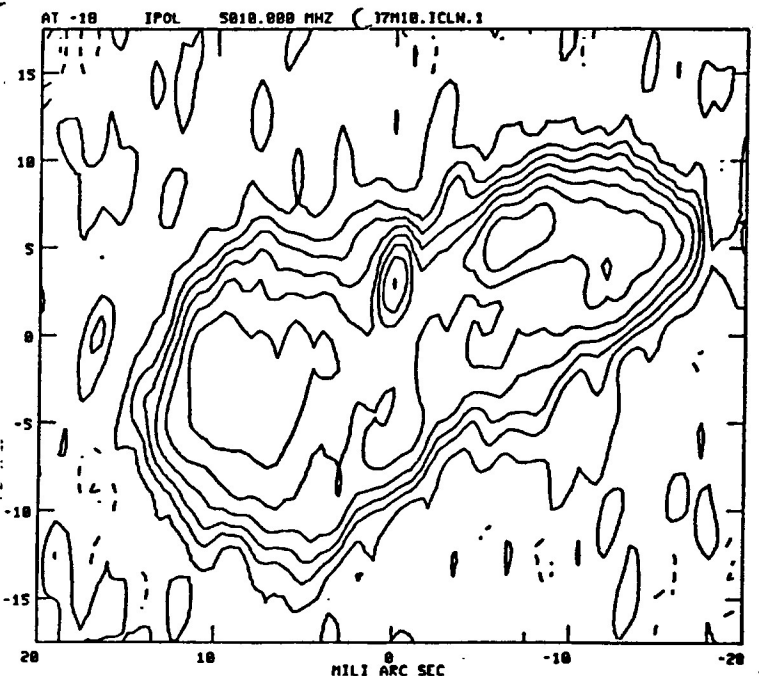
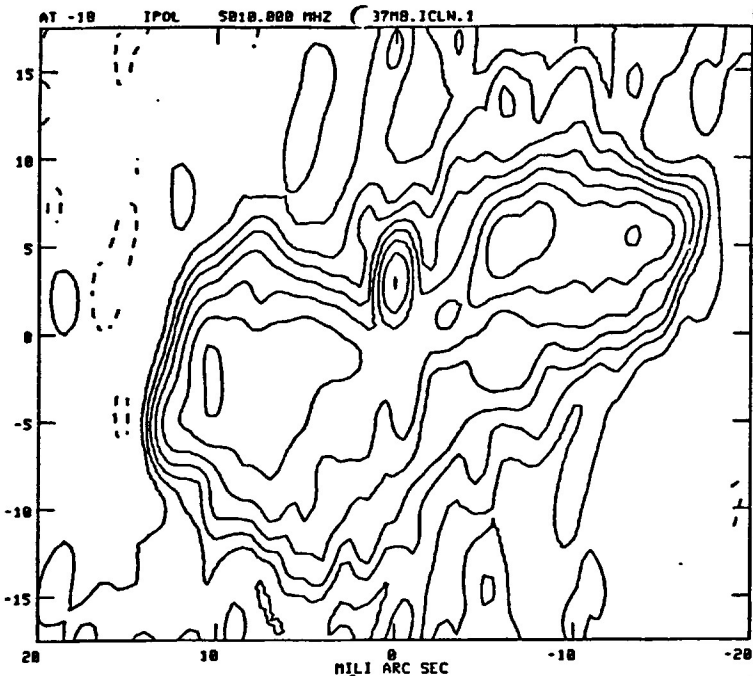
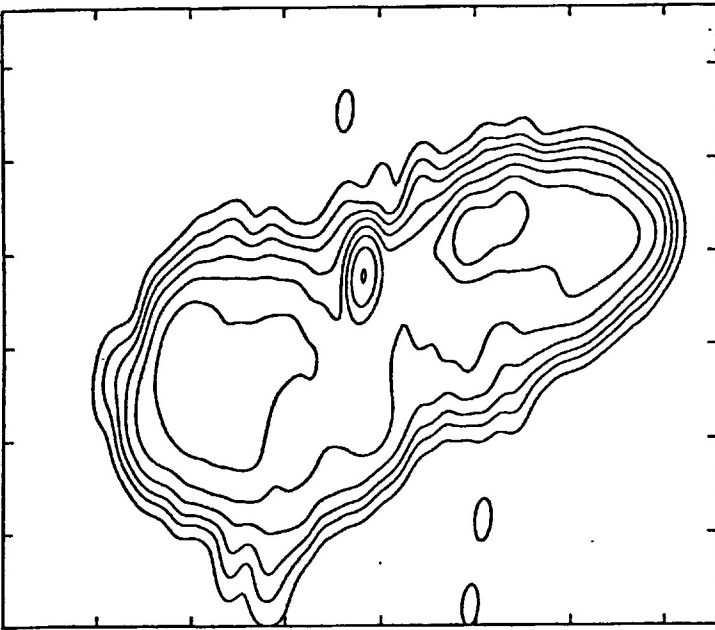
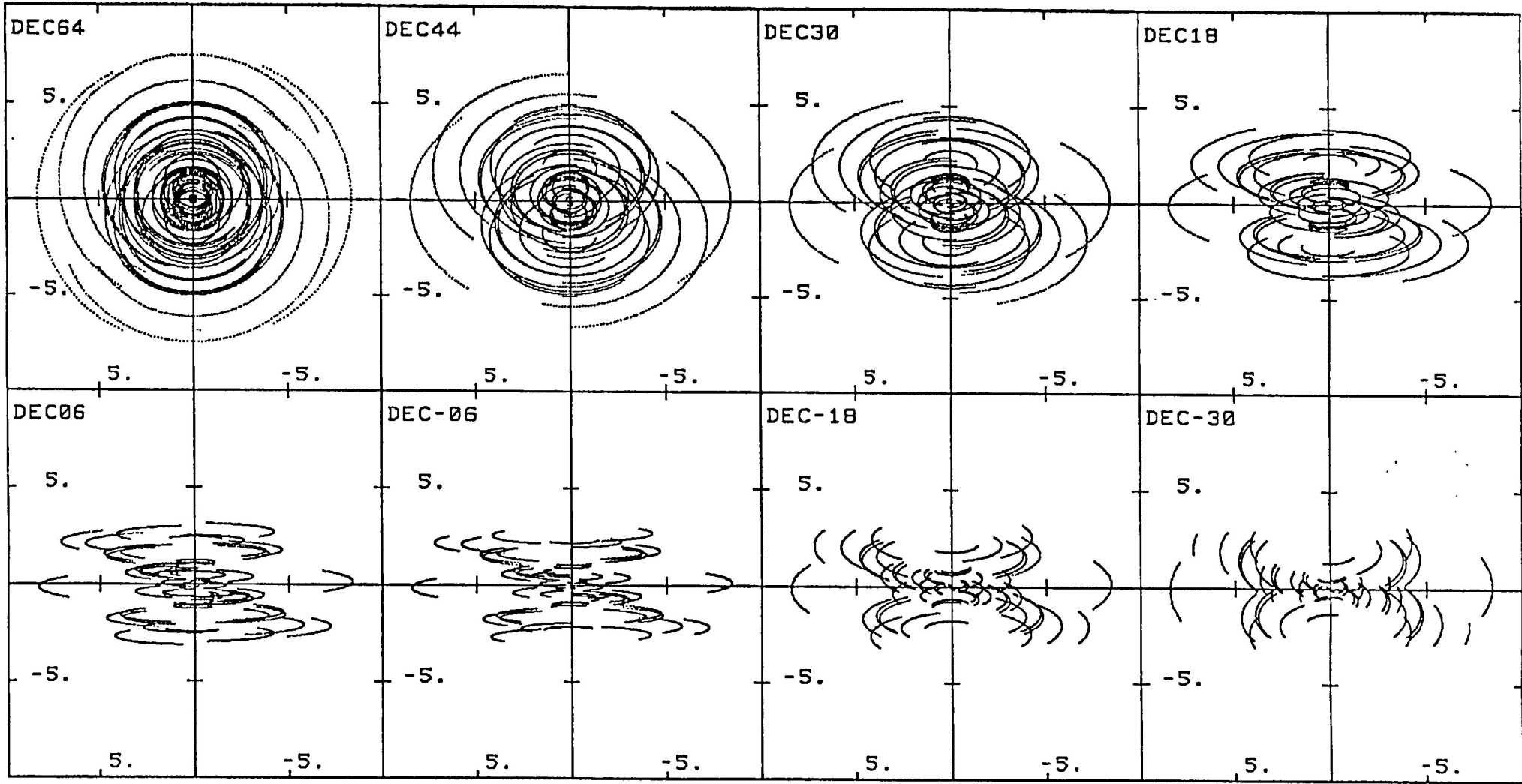


Figure III-3







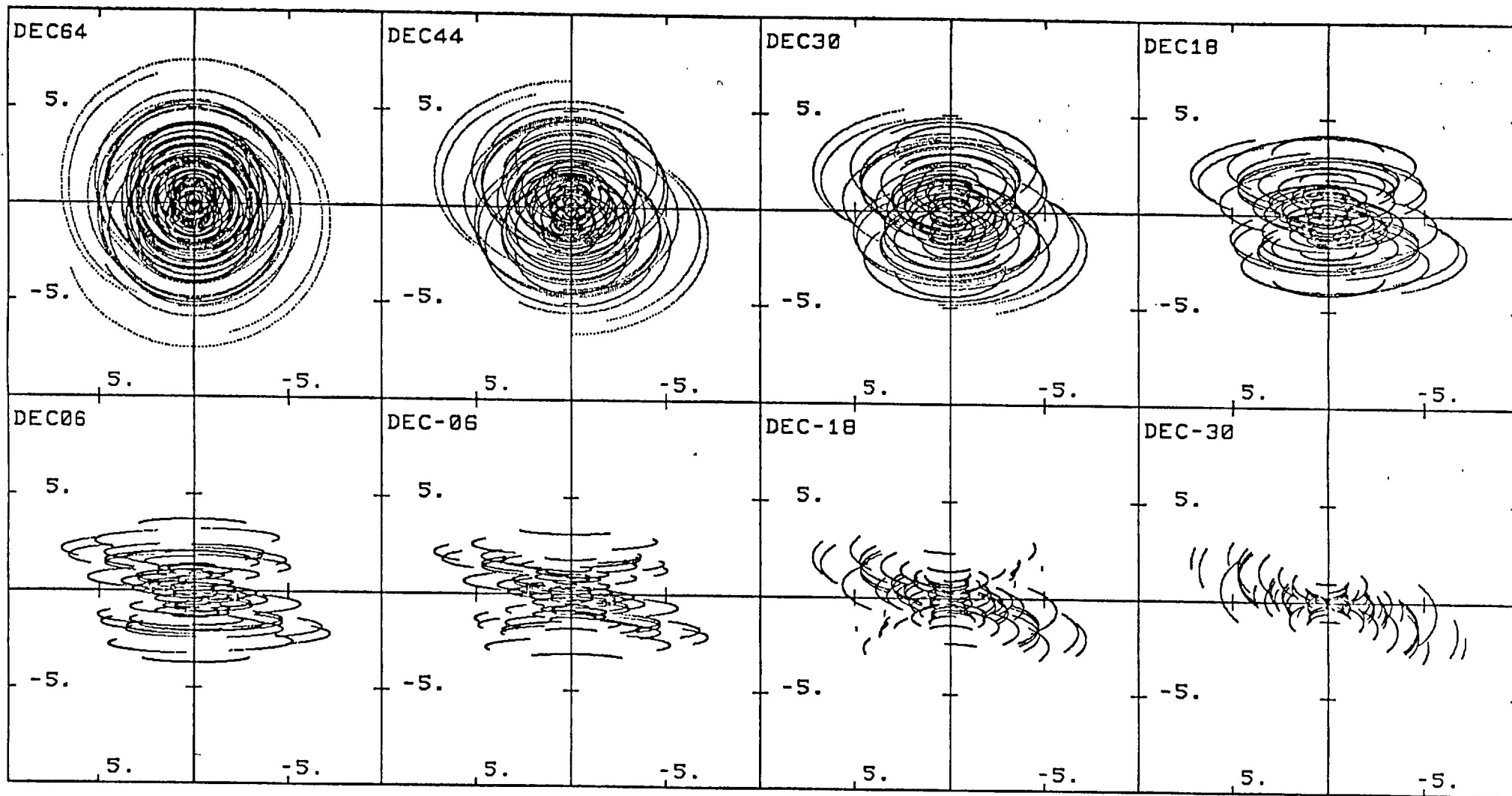
ARECIBO HAWAII GRFALL HSTK SOCORRO IOWA LUGS LUNM

0.30 MHz

(wavelengths  $\times 10^3$ )

DEC = 64.0

Figure III-4



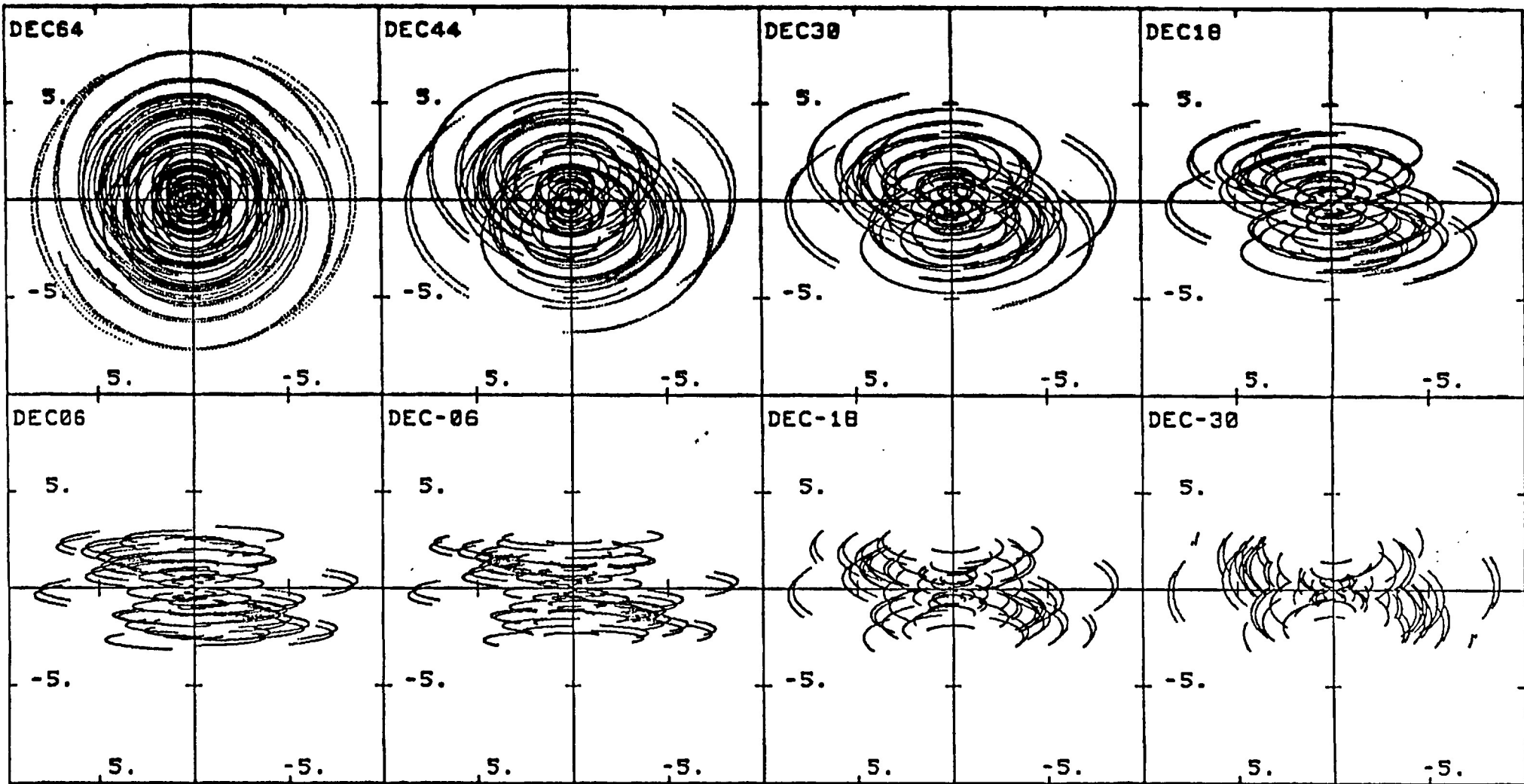
HAWAII ANCH OURO SOCORRO LASL BLDR GRFK2 NRAO HSTK BRUL2

0.30 MHz

(wavelengths  $\times 10^3$ )

DEC = 64.0

Figure III-5



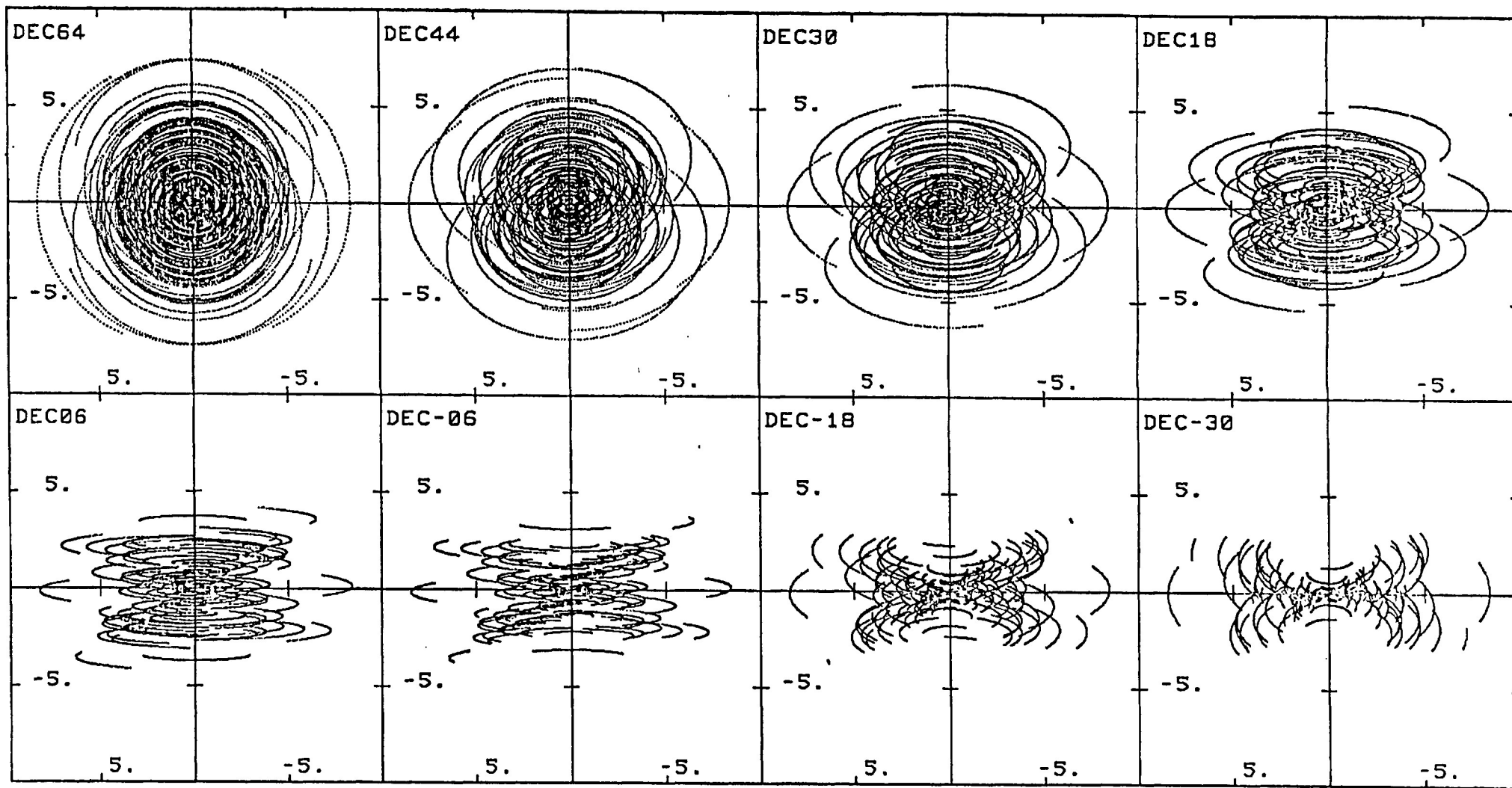
KAUAI HILO SPKN TUSCNE ULASW LRDO IOWA BANGOR ARECIBO PUEBLO

0.30 MHz

DEC = 64.0

(wavelengths  $\times 10^3$ )

Figure III-6



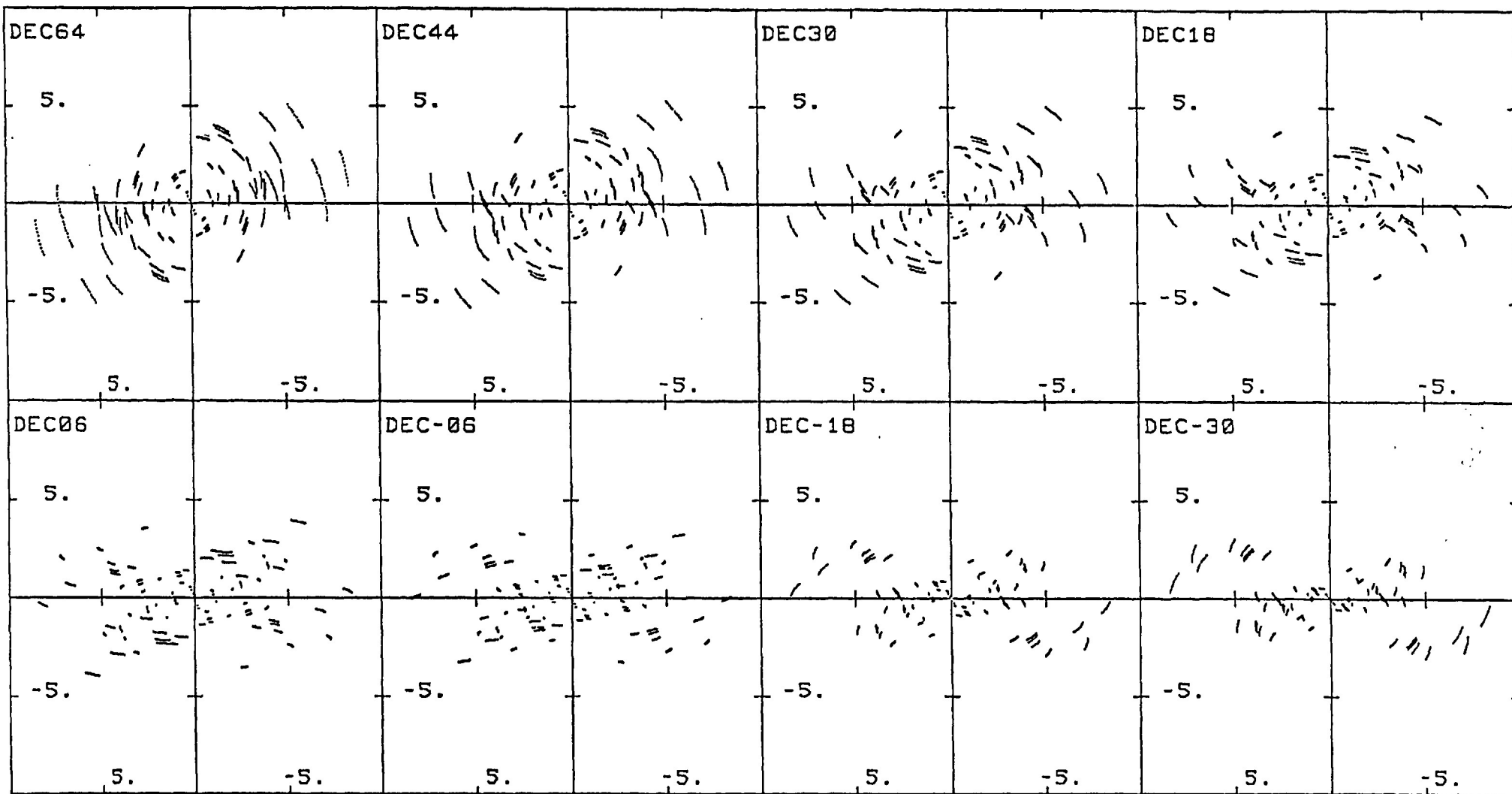
SOCORRO ARECIBO HAWAII ANCH OURO SALEM BOIS BLDR DSS14 IOWA HSTK LRDO

0.30 MHz

(wavelengths  $\times 10^3$ )

DEC = 64.0

Figure III-7



HAWAII ANCH HSTK ARECIBO OURO SOCORRO LASL DENVER GRFK2 CAPECAN

0.30 MHz

(wavelengths x 10<sup>3</sup>)

Figure III-f

DEC = 64.0 GST = 6.0, 7.0